Photoluminescence Spectral Change in Layered Titanate Oxide Intercalated with Hydrated Eu^{3+}

Shintaro Ida,* Ugur Unal, Kazuyoshi Izawa, Ozge Altuntasoglu, Chikako Ogata, Taishi Inoue, Kenji Shimogawa, and Yasumichi Matsumoto

Department of Nano Science and Technology, Graduate School of Science and Technology, Kumamoto University, Kurokami 2-39-1, Kumamoto 860-8555, Japan

Received: June 2, 2006; In Final Form: September 23, 2006

A number of interesting photoluminescence properties of titanate layered oxide intercalated with hydrated Eu^{3+} have been demonstrated. Photoluminescence intensity of Eu^{3+} decreased rapidly with time during irradiation by UV light having energy higher than the band gap energy of the host TiO ($Ti_{1.81}O_4$) layer. This is presumably due to the decrease in energy transfer from the host TiO layer to Eu^{3+} as a result of the change in the hydration state of water molecules surrounding Eu^{3+}, which is caused by the hole produced in the TiO valence band. When irradiation was discontinued, the emission intensity gradually recovered. The recovery time increased when the water in the interlayer is removed by heat treatment. This indicates that the state of interlayer water changes during irradiation and returns to its initial state after discontinuation of irradiation. The excitation spectra changed drastically at any given wavelength upon irradiation with UV light. A comparison of the excitation spectra before and after irradiation reveals that only the excitation peak at around the irradiation wavelength decreased upon irradiation, as in the case of spectral hole burning. The hydration state of water molecules surrounding Eu^{3+} presumably changes depending on the irradiation wavelength, leading to the above spectral change because the Eu/TiO film has a superlattice structure producing holes with different energies.

Introduction

Layered oxides have a unique structure composed of a two-dimensional host with a guest cation. The layered structure gives rise to a variety of interesting properties, such as superconductivity of Cu and Co host layers,[1−7] photocatalytic activity of interlayer nanospace in the decomposition of water [8−11] or intercalation-deintercalation ability utilized in battery applications.[12] We have identified several interesting properties of titanate and niobate type layered oxides. Electrochemical analyses revealed the n-type semiconducting behavior of the host nanosheet layer with photoelectrochemical response.[13] Intercalated Ag^+ species showed a clear electrochemical redox reaction of the Ag^+/Ag couple. In addition, the visible light response of the $Ru(bpy)_3^{2+}$ in the interlayer yielded a significant amount of photocurrent in Ti and Nb layered oxides.[14] These reactions are based mainly on the unique two-dimensional structure of the layered oxides.

In general, the intercalation of a desired guest cation into the interlayer of a layered oxide is carried out by soft-solution processes,[15−21] such as ion exchange reactions[15−17] and electrostatic self-assembly deposition (ESD).[14] The latter technique is superior as it allows simple and optimal intercalation of the guest cation. Various kinds of intercalated layered oxides can be easily obtained by electrostatic agglutinative action after mixing a solution of positively charged species and a colloidal solution of nanosheets. Layered oxides have attracted much attention as base materials for photo energy conversion and optical devices.

It has been reported that several types of layered oxides and TiO_2 nanoparticles doped with Eu^{3+} ions show strong emission by an energy transfer process from the host matrix to the in-matrix Eu^{3+} ions.[22−29] In our previous study,[30] it was discovered that the interlayer water molecules in the titanate layered oxide intercalated with Eu^{3+} ions strongly promote the emission of Eu^{3+} based on energy transfer from the titanate nanosheet layer to the Eu^{3+} ions, in contrast to the generally accepted view that the presence of water suppresses the emission of Eu^{3+} ions. In that case, the unique and special bonding state of water, as in hydrogen bonding in ice, seems to favor energy transfer for Eu^{3+} emission.[30] The water molecules in the interlayer are expected to impart other interesting properties in Eu^{3+} emission because of their unique bonding state.

Thus, the present study examined in detail the photoluminescence properties of Eu^{3+} ions intercalated in the interlayer of titanate layered oxides during UV irradiation. It was found that the emission intensity of Eu^{3+} ions immediately decreases upon UV irradiation and that the excitation spectrum changes dramatically, as in the case of persistent spectral hole burning (PSHB).[31−40] To the best of our knowledge, this is the first report on spectral change similar to PSHB for Eu^{3+} ions intercalated in layered oxides. In this paper, unique and interesting emission properties of the titanate layered oxide intercalated with hydrated Eu^{3+} ions are demonstrated.

Experimental Section

Materials. The starting material $Cs_xTi_{(2-x/4)}\square_{x/4}O_4$ (CTO, $\square$: vacancy) was prepared by the complex polymerization method.[16] Prior to the addition of $Ti(OCH(CH_3)_2)_4$ (10.796 mL), Cs_2CO_3 (3.4983 g) was dissolved in a mixture of methanol (160

* Corresponding author. E-mail: s_ida@chem.chem.kumamoto-u.ac.jp. Telephone: +81-96-342-3659. Fax: +81-96-342-3679.

10.1021/jp063412o CCC: $33.50
Published on Web 11/07/2006

mL) and ethylene glycol (60 mL). During the addition of titanium isopropoxide, the mixture was stirred vigorously with a magnetic stirrer and the temperature was raised gradually to 50 °C. The resultant solution was clear. Next, anhydrous citric acid (28.8 g) was added and the temperature was raised to 150 °C, yielding a resin-like mass, which transformed into ash and then into white powder upon raising the temperature to 300 °C. Calcination of the powder at 800 °C yielded the final CTO ($Cs_xTi_{(2-x/4)}\square_{x/4}O_4$, where $x = 0.76$). Thus, all Ti cations in the present CTO oxide occurred as Ti^{4+}. The average particle size was about 4.0 μm after milling. $Eu(CH_3COO)_3$ was used as the source of Eu^{3+} ions.

Protonation and Exfoliation. Protonation of the starting materials resulted in $H_xTi_{(2-x/4)}\square_{x/4}O_4 \cdot H_2O$ (HTO). Protonation was performed by stirring 5 g of CTO powder in 200 mL of 1 M aqueous HCl solution for 24 h. This sample contained only a small amount of Cs (Cs/Ti atomic ratio = 0.04). Subsequent vacuum filtration yielded the HTO powder. The HTO powders were exfoliated in an aqueous ethylamine solution. The reaction was allowed to proceed for 24 h under continuous stirring to obtain a reasonable amount of exfoliation. Subsequent centrifugation at 2000 rpm for 30 min yielded colloidal suspensions having exfoliated titanate nanosheets.

ESD Method (Preparation of Eu/TiO films). The intercalation of Eu^{3+} ions into the interlayer of titanate nanosheets was carried out using electrostatic self-assembly deposition (ESD).[9,10] The ESD method was performed by simply adding 10 mL of ethylamine colloidal solution containing titanate nanosheets into the aqueous solution of Eu^{3+} ions. The pH of the colloidal solution was carefully adjusted to 7.5−8.0 using a 0.1 M HCl solution. The initial pH values of aqueous lanthanide cation solutions were in the range 5.5−7.0, and no pH adjustment was applied to the solutions. Mixing of the two solutions immediately resulted in a precipitate consisting of a single phase of the lanthanide intercalated titanate layered oxides formed by electrostatic interaction between the negatively charged TiO_2 nanosheets and positively charged Eu^{3+} ions. The precipitate was rinsed with double-distilled water three times in order to remove excess Eu^{3+} ions and other undesired ions. To prepare films of layered oxides intercalated with Eu^{3+} ions, the precipitate was simply applied on a Pt substrate after extracting (0.2 mL) with a pipet and allowed to dry at room temperature. The average film thickness was calculated to be about 10 μm from the total amount of Ti in the film. The layered films prepared are described as Eu/TiO films. These films were heated at various temperatures for 1 h.

Characterization and Equipment. The crystal structure and orientation of the films were analyzed by X-ray diffraction (using Cu Kα radiation, Rigaku RINT-2500VHF). The compositions of the deposited films were analyzed by an inductively coupled plasma (ICP) spectrophotometer (Seiko Instruments, SPS7800) and/or X-ray photoelectron spectrometer (XPS, VG Scientific Σ-probe). The ICP was carried out after dissolving the films in HCl solution. Fourier transformed infrared spectra (FT-IR Perkin-Elmer) of the films were obtained with the KBr technique. An appropriate amount of each sample was mixed with 0.3−0.5 g of KBr and pressed into a pellet. The samples were analyzed immediately after preparing the pellets. Thermogravimetric differential thermal analysis curves were obtained by thermal analysis (Seiko TG/DTA). Excitation and emission spectra were analyzed by a Jasco FP-6500 spectrofluorometer with a 150 W Xe lamp source. Excitation and emission spectra were taken at room temperature. Excitation and emission spectra were obtained under a scan rate of 5000 nm/min and a delay time of 0.02 s. Irradiation with UV light was performed using a Jasco FP-6500 spectrofluorometer with a 150 W Xe lamp source. The time dependence curve of emission intensities of Eu^{3+} ions was obtained at a delay time of 0.02 s.

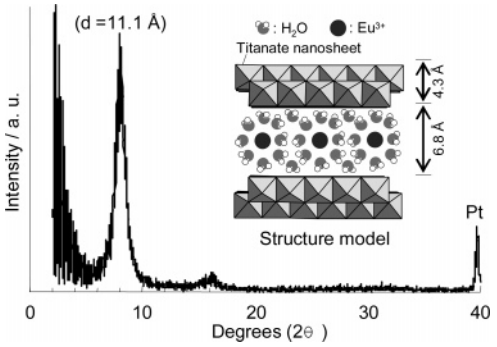

Figure 1. XRD pattern and structure model of as-deposited titanate layered oxide intercalated with Eu^{3+} ions.

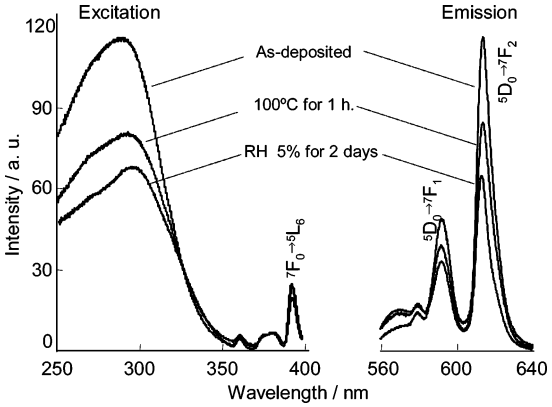

Figure 2. Room-temperature excitation ($\lambda_{em} = 614$ nm) and emission ($\lambda_{ex} = 300$ nm) spectra of Eu/TiO films treated at 100 °C for 1 h and under 5% humidity for 2 days.

Results and Discussion

Figure 1 shows the XRD pattern of an as-deposited Eu/TiO film in which Eu^{3+} ions and water molecules are sandwiched between titanate nanosheets. The interlayer distance of as-deposited Eu/TiO was 6.8 Å. The host thickness was calculated using the reported results of the X-ray structure analysis of $Cs_{0.7}Ti_{1.825}O_4$.[41] From ICP and thermal analyses (see Supporting Information Figure S1), the composition with water content was determined to be $Eu_{0.31}Ti_{1.81}O_4 \cdot 2.1H_2O$. This indicates that the intercalated Eu^{3+} ions exist as aqua ions and are coordinated with 7−10 water molecules under ambient conditions. Calculations were performed under the assumption that a significant portion of the intercalated water molecules surrounds the lanthanide cations in the interlayer because lanthanides have a high tendency of hydration in an aqueous environment. Theoretically, the negative charge of the titanate nanosheet layers may be neutralized only if 0.25 mol of Eu^{3+} is present in the interlayer of 1 mol of layered oxide according to the chemical composition of the original layered compound $Eu_{0.25}Ti_{1.81}O_4 \cdot nH_2O$. This is in close agreement with the above composition derived from the ICP measurement.

Figure 2 shows the excitation and emission spectra of Eu/TiO films before and after treatment at 100 °C for 1 h. The emission spectra were obtained under an excitation wavelength of 300 nm. The broad excitation peak at 250−350 nm in the excitation spectra is mainly the result of the band gap excitation in the titanate nanosheet layer.[29,30] The peak at 395 nm in the

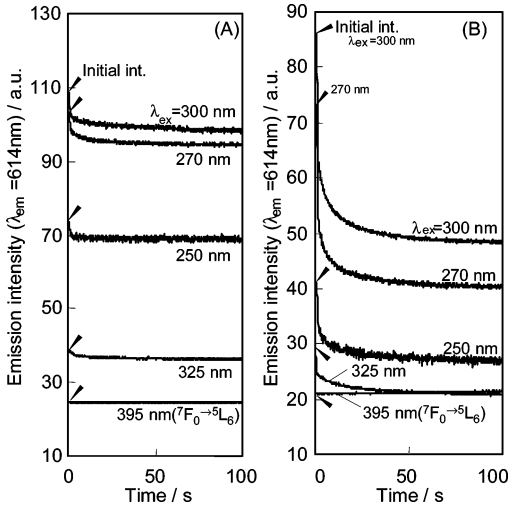

Figure 3. Time evolution of emission intensities for excitation light of varying wavelength at Eu/TiO: (A) an as-deposited sample, (B) a sample treated at 100 °C for 1 h.

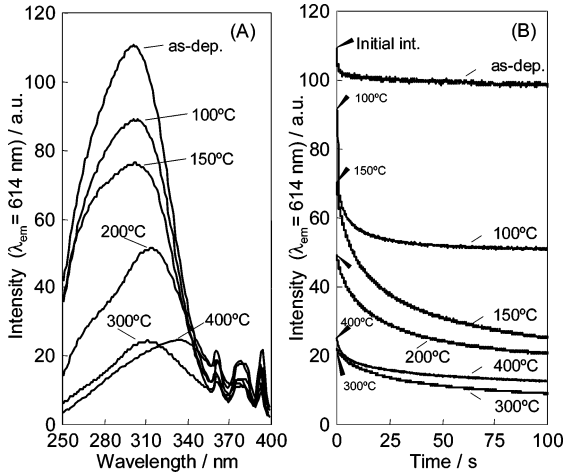

Figure 4. Excitation spectra of Eu/TiO samples treated at various temperatures (A), and the time evolution of the emission intensities during irradiation with UV light with wavelengths of the top peak in each excitation spectrum (B).

excitation spectra is due to the $^7F_0 \rightarrow {}^5L_6$ intra-4f transition of some Eu^{3+} ions adsorbed on the titanate nanosheets as an impurity.[30] The emission peaks at 593 and 614 nm are assigned to the $^5D_0 \rightarrow {}^7F_1$ magnetic dipole transition and the $^5D_0 \rightarrow {}^7F_2$ electric dipole transition, respectively. The excitation peak intensity of the as-deposited Eu/TiO film is stronger than that of the Eu/TiO film treated at 100 °C for 1 h because the amount of interlayer water that contributed to energy transfer is decreased by the heat treatment. The layer distance was decreased from 6.8 to 5.1 Å upon heat treatment at 100 °C because of the release of water molecules from the interlayer. Emission intensity and layer distance were decreased by the decrease in humidity for the same reason as illustrated in Figure 2.[30]

Figure 3 shows the time evolution of emission intensities for excitation lights with various wavelengths at Eu/TiO. Emission intensities were measured during irradiation with monochromic light of varying wavelength. For UV irradiation at a wavelength of 250, 270, 300, or 325 nm with energies higher than the band gap of the host nanosheet, the emission intensities decreased with irradiation time. In the case of UV irradiation at 395 nm, which is the $^7F_0 \rightarrow {}^5L_6$ absorption band of the impurity Eu^{3+}, no decrease was observed in the emission intensity. Thus, the emission intensity decreased during UV light irradiation, which brings about the energy transfer from TiO host layer to the hydrated Eu^{3+}. The decrease in the emission intensity was larger for the samples treated at 100 °C than for the as-deposited sample, as shown in Figure 3. According to the TG/DTA data and XRD patterns, the amount of interlayer water was less for the samples treated at 100 °C than for the as-deposited sample. These results indicate that the hydration state of the interlayer water molecules surrounding Eu^{3+} is significantly related to the decrease in emission, where the hydration state means both the number of water molecules surrounding Eu^{3+} and the configuration of the water molecules in the interlayer.

Figure 4 shows the excitation spectra (A) and the time evolution of the emission intensities (B) for Eu/TiO films treated at various temperatures. The excitation peak intensities in the range 250−350 nm assigned to the energy transfer from titanate nanosheets to the hydrated Eu^{3+} ions decreased with increasing treatment temperature. The decrease in the excitation peak intensity is due to the loss in the interlayer water. The time evolution curves of the emission intensities in Figure 4B were obtained during UV irradiation at wavelengths corresponding to the top peak on each excitation spectrum in Figure 4A. The decline in intensity over a period of 100 s was small for the as-deposited samples, while that for samples treated at 100−400 °C were relatively large. The TG/DTA data revealed that first, the relatively free water molecules in the interlayer were removed in the temperature range of RT-100 °C. The water molecules surrounding the Eu^{3+} ions, which strongly affected the energy transfer from the host nanosheets to the Eu^{3+} ions, were removed at 100−400 °C. In the case of the as-deposited sample, UV radiation might influence only a small portion of the interlayer water molecules surrounding the Eu^{3+} ions because the relatively free water molecules in the interlayer capture the holes generated, as described in a later section. Meanwhile, the samples treated at 100−400 °C are influenced by the UV radiation because the free water molecules in the interlayer have already been removed. The decrease in emission intensity of Eu/TiO film treated at 150 °C was the largest in all the samples. In the cases of Eu/TiO films treated at 200−400 °C, there was a small amount of interlayer water affecting the emission change. As a result, the change in the emission intensity is lower for the sample treated at 400 °C than for that at 100−300 °C.

In our previous study, it was confirmed that the layered structure of Eu/TiO film was kept during heat treatment in the range of 100−400 °C.[30] With regard to the stability of host layers on UV irradiation, no difference in Raman spectra for the Eu/TiO films was observed before and after UV irradiation. Consequently, the TiO host layer is stable on heat treatment below 400 °C and under UV irradiation.

Figure 5 shows the photoluminescence properties of Eu/TiO films in H_2O and D_2O. The films were treated at 100 °C before the measurement. The measurement was performed by soaking the sample films in a quartz cell filled with H_2O or D_2O at room temperature. A comparison of the excitation and emission spectra reveals that the peak intensities in D_2O were larger than those in H_2O. It is known that, in general, the excited states relax via two competitive paths. One is by light emission and the other is by phonon emission (quenching), and the latter path is important for the present case. The rate of phonon emission, ω, depends on the phonons emitted simultaneously to bridge the energy gap and is expressed as:

$$\omega \propto \exp(-k\Delta E/h\nu_{max}) \quad (1)$$

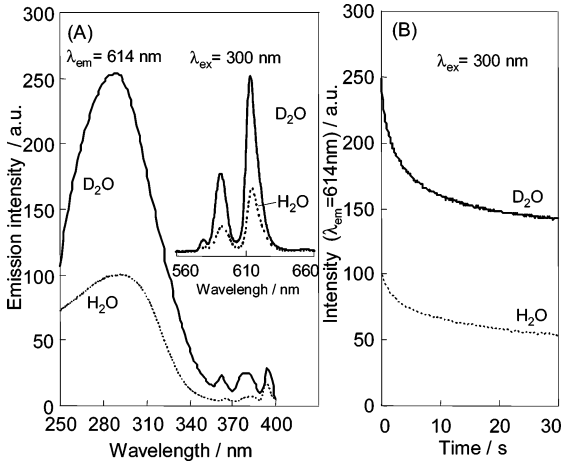

Figure 5. Excitation and emission spectra in H_2O and D_2O of Eu/TiO treated at 100 °C (A), and the time evolution of the emission intensity (λ_{ex} = 300 nm) in H_2O and D_2O at Eu/TiO treated at 100 °C (B).

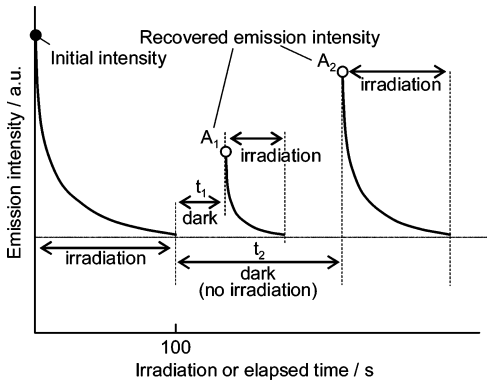

Figure 6. Models of the emission intensity as a function of elapsed time (t_1, t_2) where no irradiation is carried out (in dark). The measurement was made after 100 s of irradiation.

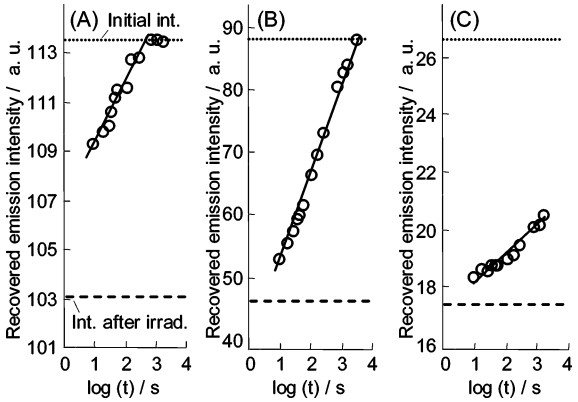

Figure 7. Recovered emission intensity as a function of elapsed time for Eu/TiO treated at various temperatures: (A) as-deposited, (B) 100 °C, (C) 400 °C.

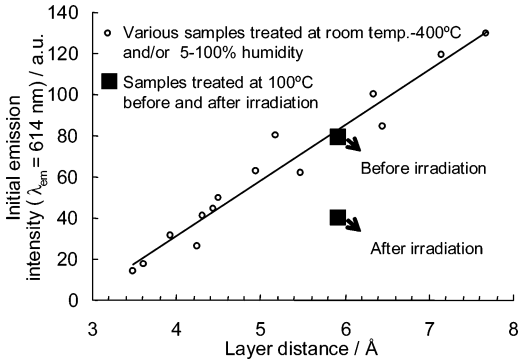

Figure 8. Initial emission intensities as a function of layer distance for samples treated at various temperatures in the RT-400 °C range and/or various humiditie (circles). The initial emission intensities and layer distances of the sample treated at 100 °C were measured at room temperature under 55% humidity before (initial intensity) and after irradiation for 100 s (squares).

where ΔE is the energy gap to the nearest lower level and is the maximum energy of phonons coupled to the emitting state. The phonon emission rate, ω, decreases rapidly with increasing ΔE, so that the competitive light emission or radiative process becomes dominant.[42−43] Large values of $h\nu_{max}$ also quench light emission. Therefore, in general, the photoluminescence of Eu^{3+} ions strongly depends on the chemical environment of the ions and Eu^{3+} ions exhibit a stronger luminescence in D_2O than in H_2O because of the smaller phonon energy of D_2O ($\nu_{O-DstretchMAX}$: ~2800 cm^{-1}) as compared to that of H_2O ($\nu_{O-HstretchMAX}$: ~4000 cm^{-1}).[44] These results revealed that the general quenching effect of Eu^{3+} emission by H_2O occurred in the interlayer. Thus, it is concluded that the photoluminescence properties of the present Eu/TiO film is dependent on the hydration state of water molecules surrounding the Eu^{3+} ions in the interlayer in the same manner with general Eu^{3+} ions in aqueous solution.

Figure 6 shows the typical model for the Eu^{3+} emission intensity of Eu/TiO film as a function of elapsed time, (t_1, t_2), in the absence of irradiation. The intensity was recovered to A_1 and A_2 after elapsed time t_1 and t_2, respectively. The recovered emission intensity depended on the elapsed times, as shown in Figure 6. In general, the emission intensity reverted to its initial intensity. The recovery of the emission intensity with time indicated that the hydration state of the water molecules surrounding the Eu^{3+} ions in the interlayer, which was altered by the UV irradiation, recovered to its initial state in the absence of irradiation. Figure 7 shows the recovered emission intensity (A shown in Figure 6) as a function of the elapsed time (t shown in Figure 6) in logarithmic scale. The measurement was carried out after 100 s of irradiation. It was found that the recovered emission intensity increased linearly on the logarithmic scale of elapsed time. The elapsed times for recovery to the initial intensity were 500 and 3600 s, respectively, for the as-deposited sample and the samples treated at 100 °C. The emission intensities for the samples treated at 400 °C did not recover to their initial intensities even after 2 days in the dark. These results suggest that the UV-altered hydration state of the water molecules surrounding the Eu^{3+} ions in the interlayer recovers more easily in the case of nonheat-treated samples or samples heat-treated at lower temperatures.

When the hydration state recovers to the initial hydration state, it may be possible that the released energy is fed to the Eu^{3+}, causing emission. The lifetimes of Eu^{3+} emission (λ: 614 nm) for Eu/TiO films before and after UV light irradiation for 100 s were 500 and 503 μs^{-1}, respectively. These values agree with the general lifetime of lanthanide emission.[45] The Eu^{3+} emission (afterglow) was not observed after 10 ms (see Supporting Information, Figure S2). In the case of the Eu/TiO film treated at 100 °C, it took about 3 h until the decreased emission intensity recovered to the initial emission intensity. Thus, the recovery of the changed hydration state is not related to the emission.

Figure 8 shows initial emission intensity as a function of layer distance for various samples. The layer distances were controlled by humidity and/or heat treatment in terms of the amount of water in the interlayer. The circles correspond to the samples treated at various temperatures (RT-400 °C) and/or humidities (5−100%). It was found that the emission intensities decreased with decreasing layer distance and hence decreasing water

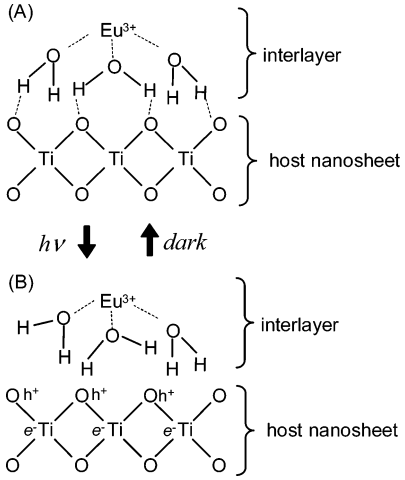

Figure 9. Model of change in the hydration state of water molecules surrounding Eu^{3+}: (A) before and (B) after irradiation.

content of the interlayer. Figure 8 also shows the results for samples treated at 100 °C before and after irradiation (data shown by the squares). From XRD and thermal analyses under UV irradiation (see Supporting Information, Figures S3 and S4), we confirmed that both the layer distance and the amount of interlayer were unchanged during UV light irradiation. The emission intensity decreased upon irradiation, but the layer distances remained unchanged. This indicates that the amount of interlayer water remained constant during irradiation and that the interlayer water did not decompose as a result of the irradiation.

As mentioned already, the mechanism for the irradiation-induced decrease in emission intensity is related to the irradiation-induced change in the hydration state of the water molecules surrounding the Eu^{3+} ions. There are several reports on the state of the hydrogen bonds on the surface of the nanosheet and TiO_2 using ^1H NMR.[46−50] Takagaki and Domen et al. reported that there are several types of OH groups in the exfoliated $HTiNbO_5$.[46,47] Nosaka et al. reported that the H_2O molecules with high mobility were increased on the TiO_2 surface by UV irradiation, and almost all of the physisorbed water on TiO_2 surface was eliminated at 150 °C.[48−50] We propose the model for the change in the hydration state by UV irradiation in Figure 9. Interlayer water molecules form weak bonds between the hydrogen atoms of H_2O and the oxygen atoms of the titanate nanosheet such as hydrogen bonds, as shown in Figure 9A. When the titanate nanosheets are irradiated with UV light at energies higher than that of the band gap energy of the nanosheets, electrons and holes are generated in the nanosheets, and the holes migrate to the electronegative oxygen atoms of the nanosheets. As a result of this migration, the bond between the hydrogen atoms of H_2O and the oxygen atoms of the titanate nanosheets might weaken and be broken because the electronegativity of the oxygen atoms in the nanosheets decreases upon trapping holes. This mechanism is illustrated in Figure 9B. Consequently, the bond cleavages between interlayer water molecules and titanate nanosheets will decrease the energy transfer, and concomitantly, the resultant free water molecules surrounding Eu^{3+} increase the symmetry around the Eu^{3+}, leading to the decrease in emission intensity. However, as for the hydration state change by irradiation, we have not obtained the evidence of rearrangement of interlayer water by irradiation yet. The difference in IR spectra before and after irradiation was not observed with FT-IR. Probably, the state change by irradiation may be very insignificant. The study about detailed mechanism is currently in progress. Hashimoto et al. have

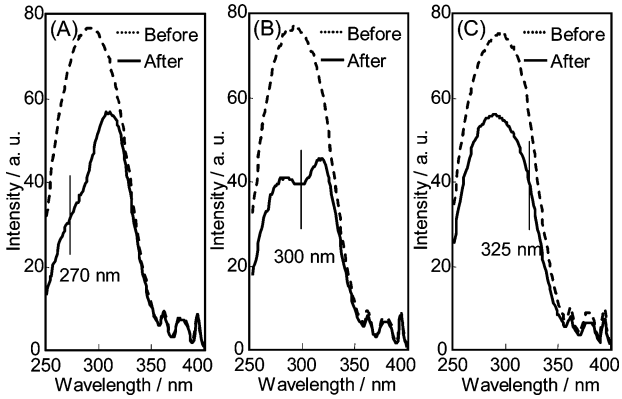

Figure 10. Excitation spectra of Eu/TiO films treated at 100 °C before and after irradiation by UV light of varying wavelength for 100 s; irradiation wavelength: (A) 270 nm, (B) 300 nm, and (C) 325 nm.

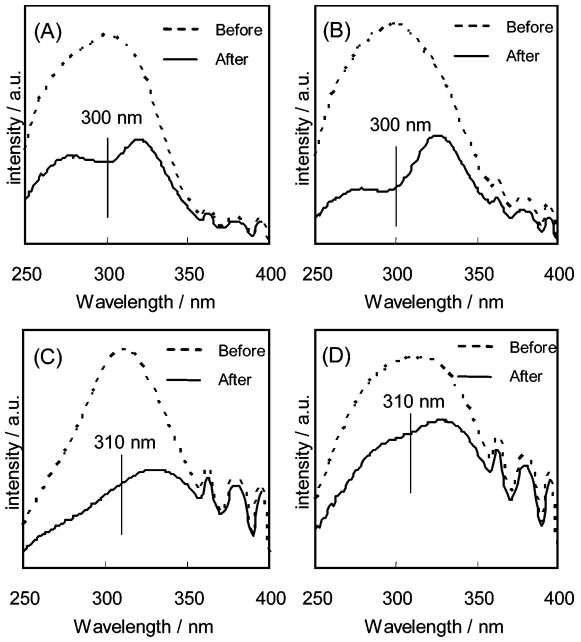

Figure 11. Excitation spectra of Eu/TiO films treated at various temperatures before and after irradiation for 100 s: (A) treatment temperature, 150 °C, irradiation wavelength, 300 nm; (B) 200 °C, 300 nm; (C) 300 °C, 310 nm; (D) 400 °C, 310 nm.

reported that irradiation of the TiO_2 surface with UV light causes rearrangement of the hydroxyl groups on the surface, and the rearrangement state is stable for several hours or more.[51,52] This is similar to the above-proposed mechanism in that hydration state is changed by UV irradiation and the changed hydration state is relatively stable.

Figure 10 shows the excitation spectra of Eu/TiO films before and after irradiation with UV light of varying wavelength at room temperature. The dotted and solid lines in Figure 10 show the spectra before and after irradiation for 100 s, respectively. It should be noted that the excitation intensity at around the wavelength in UV light irradiation was decreased as compared with that before irradiation. These spectral changes are similar to spectral hole burning. Figure 11 shows excitation spectra of Eu/TiO films treated at various temperatures before and after irradiation for 100 s. Spectral changes were observed for all samples, but the spectral changes could not be clearly resolved for samples treated at higher temperatures (300−400 °C). There are several reports on spectral hole burning related to Eu^{3+} ions. For example, Fujita et al.[31,32] and Nogami et al.[33,34,37] reported that persistent spectral hole burning (PSHB) phenomena were

observed at room temperature for glasses doped with Eu^{3+}. Hole burning is observed on the excitation spectra of the $^7F_0-^5D_0$ transition of Eu^{3+} ions, although the hole burning mechanism is still unknown. Fujita et al. reported that the mechanism for hole burning involves the photoinduced reduction of Eu^{3+} ions to Eu^{2+} ions through the release of a hole.[31,32] Nogami et al. reported that the mechanism for hole burning is related to the electron transfer between the Eu^{3+} ions and the defect centers in the matrix.[33,34,37] The above spectral change observed for Eu/TiO in the present study is presumably due to the change in the hydration state of water molecules surrounding Eu^{3+} in the interlayer. The mechanism can be explained by the layered structure of the Eu/TiO film, which resembles a superlattice structure,[53,54] because the Eu/TiO film has a structure consisting of the alternating laminated film of the TiO nanosheets layers and the guest layers. It is known that discrete levels of electron orbital are formed in the superlattice. When the Eu/TiO film is irradiated with UV light, electrons are excited to their discrete vacant energy levels (conduction levels) from occupied levels (valence levels) depending on the absorbed wavelength. In the general model of photoexcitation in a semiconductor, when an electron is excited from a deep valence level to a high conduction level, the generated electron and hole with higher energy move to the bottom of the conduction band and the valence band with relaxation, respectively. The relaxation results from the process of diffusion of the excited and continuous energy level. On the other hand, in the case of TiO nanosheets, because the thickness is very thin (0.43 nm), it is expected that the quantization of its valence and conduction bands and very fast diffusion of the generated electrons and hole to the surface occurs. The discrete energy levels and the fast diffusion of the excited carrier suppress the relaxation, which results in the generation of the electrons and holes having different energies (see Supporting Information, Figure S5). These holes will alter the hydration state of water molecules depending on their energy levels, contributing to the decrease in the energy transfer depending on the wavelength. Thus, the energy transfer between the host and the guest results in the spectral change in the excitation spectra at the corresponding wavelength. The study about the detailed mechanism in superlattice effect is currently in progress.

Conclusion

Titanate layered oxides intercalated with hydrated Eu^{3+} ions were prepared by the electrostatic self-assembly deposition method. The emission intensity of Eu^{3+} immediately decreased upon UV irradiation at energies higher than the band gap energy of the host TiO layer. The decrease in the emission intensity depended on the amount of interlayer water. A comparison of the emission spectra obtained by measurement in D_2O and H_2O revealed that the emission intensities in D_2O were larger than those in H_2O, indicating that the photoluminescence properties of Eu/TiO films are strongly dependent on the hydration state of the water molecules surrounding Eu^{3+} ions in the interlayer. The layer distances of Eu/TiO films before and after irradiation were the same, indicating that the decrease in emission intensity was not due to the decomposition of interlayer water by UV irradiation. Rather, the decrease was due to the decrease in the energy transfer from the host TiO layer to Eu^{3+} as a result of the change in the hydration state of water molecules surrounding Eu^{3+}, which is caused by the hole produced in the TiO valence band. When the irradiation was discontinued, the emission intensity recovered after a certain period of time. This indicates that the hydration state of water molecules surrounding Eu^{3+} changes under irradiation and returns to its initial state after discontinuation of irradiation. The excitation spectra changed drastically upon UV irradiation with the corresponding wavelength of UV light. Comparing the excitation spectra before and after irradiation shows that only the excitation peak at around the irradiation wavelength was decreased by irradiation, in a fashion similar to spectral hole burning. This unique phenomenon suggests that the hydration state of water molecules surrounding Eu^{3+} ions changes depending on the wavelength of the irradiation. This may be explained by the layered structure of the Eu/TiO film, which resembles a superlattice structure, producing holes at different energy levels.

Acknowledgment. This work was supported by a Grant-in-Aid for Scientific Research (no. 440, Panoscopic Assembling and High Ordered Functions for Rare Earth Materials, and no. 15350123) from the Ministry of Education, Culture, Sports, Science, and Technology.

Supporting Information Available: TG/DTA curves of Eu/TiO film, Eu^{3+} emission for the Eu/TiO films with and without UV light irradiation as a function of decay time, XRD patterns of Eu/TiO films before and after UV light irradiation, TG curve of Eu/TiO film before and after UV light irradiation, and excitation model in superlattice structure. This material is available free of charge via the Internet at http://pubs.acs.org.

References and Notes

(1) Hor, P. H.; Meng, R. L.; Wang, Y. Q.; Gao, L.; Huang, Z. J.; Bechtold, J.; Forster, K.; Chu, C. W. *Phys. Rev. Lett.* **1987**, *58*, 1891−1894.

(2) Chu, C. W.; Hor, P. H.; Meng, R. L.; Gao, L.; Huang, Z. J.; Wang, Y. Q. *Phys. Rev. Lett.* **1987**, *58*, 405−407.

(3) Ihara, H.; Sugise, R.; Hirabayashi, M.; Terada, N.; Jo, M.; Hayashi, K.; Negishi, A.; Tokumoto, M.; Kimura, Y.; Shimomura, T. *Nature* **1988**, *334*, 510−511.

(4) Sugise, R.; Hirabayashi, M.; Terada, N.; Jo, M.; Shimomura, T.; Ihara, H. *Jpn. J. Appl. Phys.* **1988**, *27*, L1709−L1711.

(5) Maeda, H.; Tanaka, Y.; Fukutomi, M.; Asano, T. *Jpn. J. Appl. Phys.* **1988**, *27*, L209−L210.

(6) Matsui, Y.; Maeda, H.; Tanaka, Y.; Horiuchi, S. *Jpn. J. Appl. Phys.* **1988**, *27*, L372−L375.

(7) Takada, K.; Sakurai, H.; Muromachi, E. T.; Izumi, F.; Dilanian, R. A.; Sasaki, T. *Nature* **2003**, *422*, 53−55.

(8) Takata, T.; Shinohara, K.; Tanaka, A.; Hara, M.; Kondo, J. N.; Domen, K. *J. Photochem. Photobiol., A* **1997**, *106*, 45−49.

(9) Takata, T.; Furumi, Y.; Shinohara, K.; Tanaka, A.; Hara, M.; Kondo, J. N.; Domen, K. *Chem. Mater.* **1997**, *9*, 1063−1064.

(10) Choy, J. H.; Lee, H. C.; Jung, H.; Hwang, S. J. *J. Mater. Chem.* **2001**, *11*, 2232−2234.

(11) Choy, J. H.; Lee, H. C.; Jung, H.; Kim, H.; Boo, H. *Chem. Mater.* **2002**, *14*, 2486-2491.

(12) Bruce, P. G. *Chem. Commun.* **1997**, 1817−1824.

(13) Matsumoto, Y.; Funatsu, A.; Matsuo, D.; Unal, U.; Ozawa, K. *J. Phys. Chem. B* **2001**, *105*, 10893−10899.

(14) Unal, U.; Matsumoto, Y.; Tanaka, N.; Kimura, Y.; Tamoto, N. *J. Phys. Chem. B* **2003**, *107*, 12680−12689.

(15) Sasaki, T.; Watanabe, M.; Komatsu, Y.; Fujiki, Y. *Inorg. Chem.* **1985**, *24*, 2265−2271.

(16) Abe, R.; Kondo, J. N.; Hara, M.; Domen, K. *Supramol. Sci.* **1998**, *5*, 229−233.

(17) Abe, R.; Hara, M.; Kondo, J. N.; Domen, K.; Shinohara, K.; Tanaka, A. *Chem. Mater.* **1998**, *10*, 1647−1651.

(18) Abe, R.; Ikeda, S.; Kondo, J. N.; Hara, M.; Domen, K. *Thin Solid Films* **1999**, *343*−*344*, 156−159.

(19) Fang, M.; Kaschak, D. M.; Sutorik, A. C.; Mallouk, T. E. *J. Am. Chem. Soc.* **1997**, *119*, 12184−12191.

(20) Kerimo, J.; Adams, D. M.; Barbara, P. F.; Kaschak, D. M.; Mallouk, T. E. *J. Phys. Chem. B* **1998**, *102*, 9451−9460.

(21) Schaak, R. E.; Mallouk, T. E. *Chem. Mater.* **2000**, *12*, 2513−2516.

(22) Bizeto, M. A.; Constantino, V. R. L.; Brito, H. F. *J. Alloys Compd.* **2000**, *311*, 159−168.

(23) Conde-Gallardo, A.; Garcia-Rocha, M.; Hernandez-Calderon, I. Palomino-Merino, R. *Appl. Phys. Lett.* **2001**, *78*, 3436−3438.

(24) Frindell, K. L.; Bartl, M. H.; Popitsch, A.; Stucky, G. D. *Angew. Chem., Int. Ed.* **2002**, *41*, 959−962.
(25) Frindell, K. L.; Bartl, M. H.; Robinson, M. R.; Bazan, G. C.; Popitsch, A.; Stucky, G. D. *J. Solid State Chem.* **2003**, *172*, 81−88.
(26) Kudo, A.; Kaneko E. *Chem. Commun.* **1997**, 349−350.
(27) Kudo, A.; Kaneko, E. *Microporous Mesoporous Mater.* **1998**, *21*, 615−620.
(28) Constantino, V. R. L.; Bizeto, M. A.; Brito, H. F. *J. Alloys Compd.* **1998**, *278*, 142−148.
(29) Xin, H.; Ma, R.; Wang, L.; Ebina, Y.; Takada, K.; Sasaki, T. *J. Appl. Phys. Lett.* **2004**, *85*, 4187−4189.
(30) Matsumoto, Y.; Unal, U.; Kimura, Y.; Ohashi, S.; Izawa, K. *J. Phys. Chem. B* **2005**, *109*, 12748−12754.
(31) Fujita, K.; Tanaka, K.; Yamashita, K.; Hirao, K. *J. Lumin.* **2000**, *87*−*89*, 682−684.
(32) Fujita, K.; Tanaka, K.; Hirao, K.; Soga, N. *J. Opt. Soc. Am. B* **1998**, *15*, 2700−2705.
(33) Nogami, M.; Hayakawa, T.; Ishikawa, T. *Appl. Phys. Lett.* **1999**, *75*, 3072−3075.
(34) Nogami, M. *J. Non-Cryst. Solids* **1999**, *259*, 170−175.
(35) Ricard, D.; Beck, W.; Karasik, A. Y.; Borik, M. A.; Arvanitidis, J.; Fotteler, T.; Flytzanis, C. *J. Lumin.* **2000**, *86*, 317−322.
(36) Chung, W. J.; Heo, J. *Appl. Phys. Lett.* **2001**, *79*, 326−328.
(37) Nogami, M.; Ishikawa, T. *Phys. Rev. B: Condens. Matter Mater. Phys.* **2001**, *63*, 104205/1−104205/6.
(38) Murase, N.; Nakamoto, R.; Matsuoka, J.; Tomita, A. *J. Lumin.* **2004**, *107*, 256−260.
(39) Kalluru, R. R.; Schoolfield, E.; Rami Reddy, B. *J. Appl. Phys.* **2003**, *94*, 2139−2141.
(40) Hanzawa, H.; Ueda, D.; Adachi, G.; Machida, K.; Kanematsu, Y. *J. Lumin.* **2001**, *94*−*95*, 503−506.
(41) Grey, I. E.; Li, C.; Madsen, I. C.; Watts, J. A. *J. Solid State Chem.* **1987**, *66*, 7−19.
(42) Shionoya, S., Yen, W. M., Eds.; *Phosphor Handbook*; CRC Press LCC: Boca Raton, FL, 1999; p 179.
(43) Riseberg, L. A.; Moos, H. W. *Phys. Rev.* **1968**, *174*, 429−438.
(44) Kropp, J. L.; Windsor, M. W. *J. Chem. Phys.* **1965**, *42*, 1599−1608.
(45) Barasch, G. E.; Dike, G. E. *J. Chem. Phys.* **1965**, *43*, 988−994.
(46) Takagaki, A.; Sugisawa, M.; Lu, D.; Kondo, J. N.; Hara, M.; Domen, K.; Hayashi, S. *J. Am. Chem. Soc.* **2003**, *125*, 5479−5485.
(47) Takagaki, A.; Yoshida, T.; Lu, D.; Kondo, J. N.; Hara, M.; Domen, K.; Hayashi, S. *J. Phys. Chem. B* **2004**, *108*, 11549−11555.
(48) Nosaka, A. Y.; Fujiwara, T.; Yagi, H.; Akutsu, H.; Nosaka, Y. *Chem. Lett.* **2002**, *31*, 420−421.
(49) Nosaka, A. Y.; Kojima, E.; Fujiwara, T.; Yagi, H.; Akutsu, H.; Nosaka, Y. *J. Phys. Chem. B* **2003**, *107*, 12042−12044.
(50) Nosaka, A. Y.; Nishino, J.; Fujiwara, T.; Ikegami, T.; Yagi, H.; Akutsu, H.; Nosaka, Y. *J. Phys. Chem. B* **2006**, *110*, 8380−8385.
(51) Sakai, N.; Fujishima, A.; Watanabe, T.; Hashimoto, K. *J. Phys. Chem. B* **2001**, *105*, 3023−3026.
(52) Sakai, N.; Fujishima, A.; Watanabe, T.; Hashimoto, K. *J. Phys. Chem. B* **2003**, *107*, 1028−1035.
(53) Nozik, A. J.; Thacker, B. R.; Olson, J. M. *Nature (London)* **1985**, *316*, 51−53.
(54) Nozik, A. J.; Thacker, B. R.; Turner, J. A.; Peterson, M. W. *J. Am. Chem. Soc.* **1988**, *110*, 7630−7637.